Characterization of reverse martensitic transformation in cold-rolled austenitic 316 stainless steel

Javier Fava [1,2], Cristina Spinosa [1], Marta Ruch [1], Fernando Carabedo [1],
Mónica Landau [1], Guillermo Cosarinsky [1], Adriana Savin [3],
Rozina Steigmann [3], Mihail Liviu Craus [3,4]

[1] Departamento de Ensayos No-Destructivos, CNEA, Av. Gral. Paz 1499, San Martin, Buenos Aires, Argentina
e-mail: fava@cnea.gov.ar; spinosa@cnea.gov.ar; ruch@cnea.gov.ar; fernandocarabedo@cnea.gov.ar; landau@cnea.gov.ar; cosarinsky@cnea.gov.ar
[2] Facultad Regional Haedo, UTN, Paris 532, Haedo, Buenos Aires, Argentina.
[3] National Institute of R&D for Technical Physics, Mangeron Boulevard 47, Iasi, Romania.
e-mail: asavin@phys-iasi.ro; steigmann@phys-iasi.ro
[4] Joint Institute for Nuclear Research, 6 Joliot-Curie, Dubna, Russia.
e-mail: kraus@nf.jinr.ru

ABSTRACT

In this work the reversion of the strain-induced α'-martensite to γ'-austenite was studied in a series of AISI 316 stainless steels (SS) specimens. The samples were submitted to 63% reduction in thickness by rolling at a temperature of -70ºC, to achieve high martensite content. The reversion of martensite to austenite was made by means of isochronic, isothermal heat treatments at temperatures between 200 and 900ºC, so as to induce partial martensite-austenite phase transformation. The samples were studied by optical and electronic microscopy, X-ray diffraction, magnetization measurements, microhardness, and electromagnetic non destructive methods: feritscope, conductivity measurements using Van der Pauw's technique, and magnetic permeability assessments by an eddy current inverse method.

The metalography study showed an α' lath martensite type structure and a similar one for the reverted austenite (γ'). Magnetization measurements and magnetic permeability showed that the reversion is active between 400 and 800°C. From the magnetic saturation measurements, a new calibration curve for the assessment of %α' through the feritscope readings was obtained. The results of the different techniques were compared, in order to assess the scope of the studied techniques in the characterization of rolled SS products, and in the evaluation of progress of reversion reaction.

Keywords: Martensite, reversion, austenitic, eddy current.

1. INTRODUCTION

Metastable austenitic SS of the AISI 300 series can undergo a deformation-induced martensitic (DIM) transformation: the gamma-austenite phase transforms to epsilon-martensite and to alpha'-martensite phases due to plastic deformation. The strain-induced martensitic transformation enhances the work hardening of these SS, and affects their ductility. The degree of hardening is limited by the structural stability of the material. This transformation is very important in austenitic stainless steels where the induced plastic deformation provides a combination of good mechanical properties, such as formability and strength. The extent of the martensitic transformation these steels can undergo is a function of material composition, processing temperature and strain. During cold rolling, for these steels, the most likely phase transformation is from γ-austenite (fcc) to α'-martensite (bcc or bct). Besides, by heat treatments (HT) above the As (the temperature at which the (α'$\rightarrow\gamma$) transformation starts on heating) the austenitic structure can be recovered; and the amount of reversal being related to the temperature of HT, the initial deformation-induced martensite content, and the steel grade. When the HT temperature equals A_F (end of austenization temperature) 100% austenite should be obtained; however the amount of new phase depends not only on temperature but also on the soaking time. However, the difficulty of predicting the material behaviour is one of the major drawbacks of these steels. In order to understand this behaviour it is of great importance to be able to characterize the morphology, crystallography and the amount of different types of phases.

On the other hand, the reverse martensitic transformation has received renewed attention due to the possibility to control microstructure, to obtain ultra-fine grain size in austenitic stainless steels [1], or to produce local areas of austenite in a martensitic structure for good formability with a maintained high strength [2].

Some authors HEDSTRÖM [3] and KNUTSSON, *et al.* [4] consider that the reversion of α' martensite to austenite is also a martensitic transformation. Actually the reverse austenite (γ') resembles a martensitic structure (fcc martensite), in that it is highly faulted. Though both variants (γ and γ') have the same crystal structures, the reverse martensitic transformation has a significantly different metallographic structure from that of the solution-treated austenite, if the recrystallization temperature of the austenite is higher than the martensite reversion temperature. This reversed austenite is quite imperfect, containing high concentrations of tangled and jogged dislocations with interspersed loops. The dislocation densities are about a factor of 10 greater than those observed in "normal" retained austenite [5,6]. The introduction of the complex dislocation configurations by the reversed martensitic transformation is considered to cause the marked strengthening of austenite subjected to cyclic martensitic transformation [7].

2. MATERIALS AND METHODS

2.1 Material

The specimens were cut from a sheet of AISI 316 austenitic stainless steel with a weight % composition of C 0.05%, Mn 1.04%, Si 0.60%, Ni 11.48%, Cr 16.16%, Mo 2.08%, Nb 0.015% and Fe (to balance). They were submitted to a one hour initial annealing at 1050 ºC in vacuum and cooled in air. All specimens were subsequently 63% cold rolled at −70ºC (200K) in order to induce γ→α' phase transformation, producing a maximum proportion of martensite for the steel under study [8]. This is the initial condition for the studies of the reversion of martensite. Cold-rolled specimens (65 x 30 x 2.3 mm^3) were individually submitted to HTs for the partial recovery of the γ phase. These HTs consisted of one hour soaking at temperatures between 200 and 900ºC. Thus, the austenitic γ phase was partially recovered and series of single-phase or two-phase specimens with different martensite content were obtained [8].

Small sections for metallography were cut from the large specimens. Each piece was embedded in epoxy resin, abraded with emery paper, polished with diamond paste on cloth and electropolished at 32 V in an electrolyte consisting of 90% butylcellosolve and 10% perchloric acid for 30 seconds at room temperature (RT). Microstructure was revealed by electrolytic etching at 3 V in a mixture of 50 % distilled water and 50 % HNO_3 for 5 to 7 seconds depending on the specimen. The resulting microstructures were observed by optical microscopy (OM) and scanning electron microscopy (SEM). Vickers 0.1 microhardness was measured on selected metallographic samples. The phases present in the specimens were identified by XRD (Cu K$_\alpha$ radiation).

2.2 Conductivity measurement using van der Pauw's method

A current injection method by van der Pauw [9] was selected for the measurements of conductivity (σ). It is a four-point method which can be applied to the measurement of σ of specimens having parallel faces and no holes. Current is injected through two points in the specimen; the corresponding voltage drop is measured between the other two points. A device satisfying the conditions established in VAN DER PAUW [9] was constructed for the experiments [10]. The 11.00±0.05 A current, produced by a direct current Sorensen DLM 20-30 source, was used throughout. Voltage drop was measured with a Keithley 2182 A nanovoltmeter. During the experiments, RT and sample temperature (ST) were measured. Mean RT was 19.2±0.5°C; mean ST was 27±3°C. This 6°C thermal amplitude accounts for an approximate 1.4% uncertainty in the calculated σ values, according to the tabulated thermal coefficient of resistivity for iron. The variation in the current from the direct current source determines an uncertainty in σ of about 0.9%. The uncertainty introduced by voltage measurement was much lower than the other two and was not considered. Hence the total uncertainty in σ is 1.5%.

2.3 Measurement of the relative magnetic permeability using eddy currents

In eddy current (EC) alloy characterization, material properties are inferred from the impedance of the test coil. For ferromagnetic materials, if the property under study produces a change in the magnetic permeability of the specimen, a model which accounts for this variation is necessary. The assessment of a ferromagnetic phase in an austenitic stainless steel refers not only to the presence of DIM; the same analysis techniques can

be used to study delta ferrite, an issue of great interest in the nuclear industry and others which use pressure vessels and piping of austenitic stainless steels.

The relative magnetic permeability was determined by means of the same inverse EC technique used in COSARINSKY, *et al.* [11] for non-ferromagnetic alloys and in RUCH, *et al*. [12] for ferromagnetic materials. The procedure makes a non-linear least square fitting of experimental ($\Delta Z^{E,N}$) and theoretically calculated ($\Delta Z^{T,N}$) normalized impedance change values of an EC coil on the specimens under study. The experimental measurements are made at test frequencies f_k with k=1, 2,...N (N=31 in the present case, with $f_1 = 1\ kHz$ and $f_N = 1\ MHz$). The theoretical model solved for $\Delta Z^{T,N}$ is the well-known problem of Figure 1, where all the parameters accounting for impedance change, namely geometry of coil and conductive specimen, test frequencies f_k, electromagnetic properties of the material σ and μ_r and gap between coil and conductor, lift-off z_1 are considered.
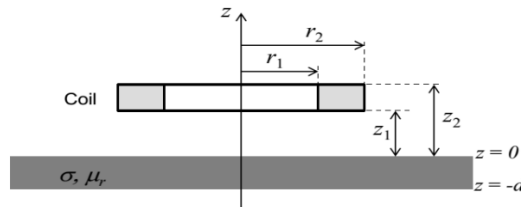
Figure 1: Electromagnetic problem.

As it is common in least square fitting, a function χ^2 to be minimized is needed; this function was constructed with the imaginary part of the complex normalized impedance changes ($(\text{Im}(\Delta Z^{E,N})$ and $\text{Im}(\Delta Z^{T,N})$): $\chi^2\left(\mu_r\right) = \sum_{k=1}^{31}\left\{\left[\text{Im}(\Delta Z^{E,N}(k)) - \text{Im}(\Delta Z^{T,N}(k))\right]^2 \Big/ \left(W_k\right)^2\right\}$. The weight functions W_k were selected as estimators of the standard uncertainty of the corresponding measurements $\text{Im}(\Delta Z^E(k))$. The estimators were calculated following the procedure indicated in COSARINSKY, *et al.* [11].

2.4 Magnetic measurements

The feritscope is an in-situ non-destructive electromagnetic EC technique. The changes in the magnetic field, which induce a voltage in a secondary coil, are related to the magnetic constituents of the material. This voltage signal is calibrated with a set of standard samples. All the magnetic components in the material can be quantified, including α-ferrite, δ-ferrite, and α'-martensite. In this work, the α' mass % content was determined with a feritscope FMP30 and a set of standards from Fischer®. As the feritscope is designed to assess the δ-ferrite content, readings must be converted by using a calibration curve. Several calibration curves have been proposed, based on different measurement techniques. A good comparison of procedures for measuring content of DIM in austenitic steels is that by TALONEN *et al.* [14]. Detailed studies of martensite measurement methods [2, 10, 14] show that feritscope readings (%δ) above 50% should be discarded, especially for cold rolled material, and that all lower readings should be multiplied by the factor 1.7 to account for true martensite content.

In order to investigate this limitation and if possible construct a new calibration curve for our 316 material, magnetic saturation measurements were undertaken. With these saturation values, it is possible to determine the magnetic moment in a specimen and to calculate the content of magnetic phase. Given the saturation magnetization for Fe (222 emu/g) and for Ni and Cr in a Fe matrix (133 emu/g and 0 to -75.2 emu/g respectively) [15], and the composition of the steel; the saturation magnetization for a 100% magnetic phase (α' in this case) can be calculated quite easily. The greatest uncertainty of the method lies in the magnetic moment of the non-Fe elements in a Fe matrix (Ni and Cr in this case), which is not very large. It is expected, this new calibration curve could be used in the assessment of α' mass % of other austenitic SS with contents of Fe, Cr and Ni similar to those of the 316 samples studied here.

Magnetic saturation measurements were made on some of our specimens with a Versalab vibrating sample magnetometer from Quantum Design, in a maximum magnetic field of 30 kOe and at a temperature of 27 °C. First saturation measurements for calibration were made on 5 of the AISI 304 steel specimens characterized in RUCH, *et al*. [2], with an α' content in the range 1.5 to 82 %, and the magnetization of each specimen was calculated. Then, saturation measurements were made on 3 of the nine 316 samples studied here. The "true α' content" was obtained as the quotient between the measured specific magnetization and

the 100% value (153-167 emu/g; mean value=160 emu/g). These values and the corresponding feritscope readings were used to construct a new calibration curve, which can be considered equivalent to that by TALONEN *et al.* [14]; but the present fitting was made with a negative exponential curve, which allows the inclusion of feritscope readings greater than 50%. The non-linear regression formula is: $y = y_0 + A \cdot \exp(R_0 \cdot x)$, with $y = \%\alpha'$ and $x = \%\delta$ reading. The constants of the fitting curve turn out to be: y_0=108; A=-108 and R_0=0.020. The quality of the fitting is reflected in that R^2=0.99521. When evaluating α' content with this curve, the uncertainties coming from the saturation magnetization measurements and from the %δ-ferrite readings must be considered.

3. RESULTS

3.1 Quantitative and qualitative results

In all the XRD diagrams it was possible to identify the peaks of α' (bcc), γ (fcc) and some very low intensity peaks which might be attributed to chromium carbides [13].

The quantitative results for the AISI 316 samples are presented in Table 1. The first column shows the specimen identification; the second column, the temperature of the reversion HT; the third, the RT electrical conductivity measured with van der Pauw's method and the fourth, the RT relative magnetic permeability as determined with the method described in Section 2.3. Column 5 shows the feritscope raw-data (%δ-ferrite as read from the equipment), and the sixth column the α' mass % content calculated according to TALONEN *et al.* [14]. Column 7 contains, the α' mass % content determined with the non-linear calibration curve from Section 2.4, and column 8, the Vickers 0.1 microhardness of the specimens, measured on the rolled face.

Table 1: Summary of results.

SAMPLE	TEMP. HT [°C]	σ [MS/m]	μ_r	%δ-FERRITE	MASS%α' [14]	MASS%α' FIT	HV 0.1
M1	200	1.20±0.02	6.2±0.2	18.2±0.6	31±1	34±2	428±41
M2	300	1.23±0.02	5.8±0.2	16.7±0.5	28.7±0.9	32±1	476±48
M3	400	1.26±0.02	5.3±0.2	15.4±0.5	26.2±0.9	29±1	503±52
M4	500	1.28±0.02	2.75±0.06	9.2±0.6	16±1	19±1	487±50
M5	600	1.28±0.02	1.83±0.03	5.5±0.3	9.4±0.5	12±1	491±51
M6	700	1.33±0.02	1.35±0.01	2.7±0.2	4.6±0.3	6±0.4	438±43
M7	800	1.36±0.02	1.29±0.01	2.1±0.1	3.6±0.2	5±0.4	433±42
M8	860	1.34±0.02	1.150±0.009	1.0±0.1	1.8±0.1	2±0.2	444±44
M9	900	1.31±0.02	1.109±0.007	0.9±0.1	1.5±0.1	2±0.2	413±39

Figure 2(a) illustrates the %α' calculated with the non-linear regression curve in Section 2.4 and the RT μ_r (columns 7 and 4 in Table 1 respectively) vs. temperature of HT. The %α' curve shows that the steepest decrease takes place for the HT at 400 to 700ºC and again the HT at 800 and 860ºC. These intervals might contain the A'$_S$ and A'$_F$ temperatures.
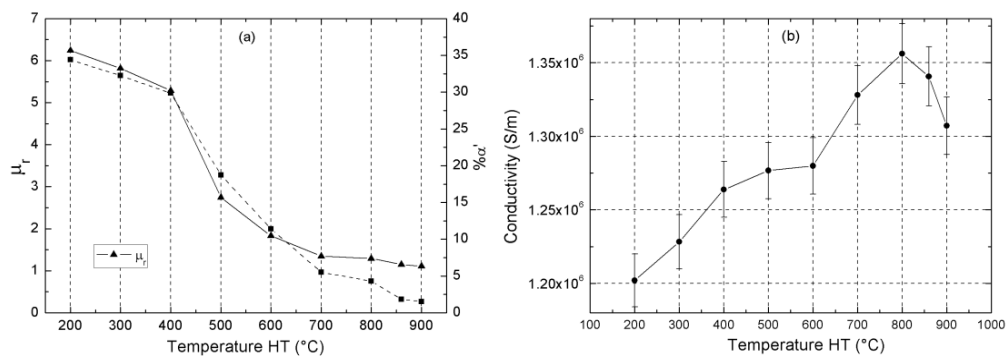
Figure 2: (a) %α' (squares) and relative permeability (triangles) vs temperature of HT. (b) conductivity vs. temperature of HT.

RT μ_r decreases monotonically with HT temperature, indicating a decrease in the magnetic phase in the specimens. An increase in RT σ is observed in Figure 2(b) in the specimens treated up to 800ºC (M7), while a decrease is observed in those treated at 860 and 900ºC. This result was also observed in the 304 SS [12].

3.2 Metallography

The evolution of the microstructure as the reversion transformation proceeds is observed in Figure 3, where (a) and (b) show images of M1 and M4 (HT at 200 and 500°C); (c) and (d), images of M8 and M9 (HT at 860 and 900 °C). All the specimens have austenite grains elongated in the rolling direction, which would indicate that the texture in the material could be conserved even after the high temperature HT. Two types of microstructures are observed. In specimens up to M6 (700°C), α' lath martensite is observed, even after an increase in the amount of reversed austenite γ' for higher temperatures. The microstructure of γ' is very similar to that of α' KNUTSSON *et al.* [6], both exhibiting a highly faulted structure, particularly so if heat treated below recrystallization temperature. From M7 on (HT temperature > 700ºC) the α' lath martensite structure is gradually replaced by a finer microstructure, possibly having less defects. Future experiments using different XRD techniques could help ellucidate these questions.
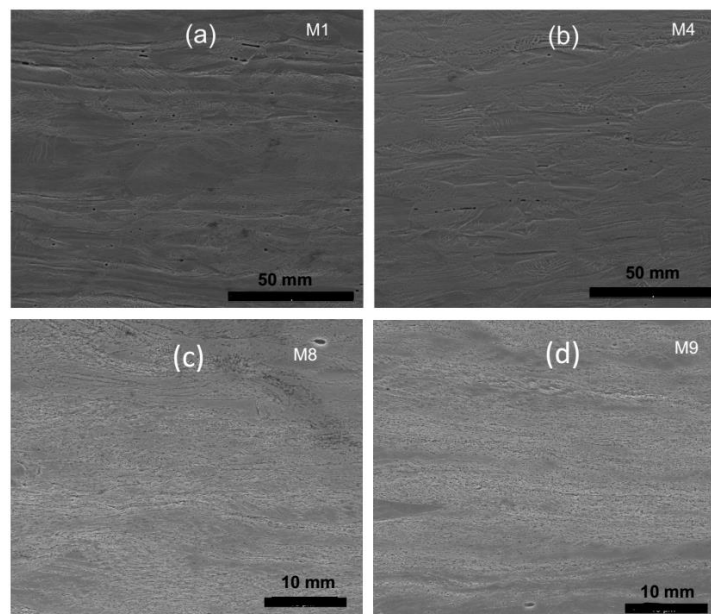
Figure 3: SEM images. (a) M1: 200°C, 33%α'; (b) M4: 500°C, 18%α; (c) M8: 860°C, 1.8%α'; (d) M9: 900°C, 1.5%α'. Cuts: (a) and (b) cross section perpendicular to the rolling direction; (c) and (d) rolled face.

4. DISCUSSION

In specimens M1 to M4 there is no apparent change in the microstructure. The alloy might be in an early stage of recovery, during which point defects are being eliminated and the annihilation and rearrangement of dislocations is still incipient. The μ_r and σ of the alloys account for the changes taking place. The former is only affected by the amount of magnetic phase present while the latter is affected by defect annihilation, dislocation rearrangement, the creation of new grain boundaries and the increase of carbon content in the matrix. In the micrographs of M1 and M4, α' lath martensite is clearly observed. From M7 on, a finer microstructure with fewer defects is observed; more marked in M8 and M9. The structure of these specimens, submitted to higher temperatures, indicate a smaller amount of defects, which may delineate textured austenitic grains in regions where at lower HT temperatures thicker α'-martensite was observed. This coincides with the decrease in conductivity.

The amount of α' is minimum for HT temperatures 860 and 900°C, as are the μ_r. These results confirm that the effective μ_r is indicative of the amount of magnetic phase. The same applies to the feritscope measurements, which is also an EC technique. The interpretation of μ_r as an EC effective parameter is the consequence of the interaction of an electromagnetic wave with a conductor.

From Figure 2 (a), it is clear that the α'→γ' transformation takes place in the range 400 to 800ºC and

there is always some retained α'. The complete reversion would only be achieved after longer HTs [6]. Many of the previously studied 304 specimens [2] had the same microstructure as that observed in M8 and M9. However, incipient recrystallization was observed in specimens of 304 heat treated at 800ºC. Hence, it can be said that M7, M8 and M9 still have a γ'-martensite-like structure, with less defects than those submitted to HT at lower temperatures, and apparently recrystallization was not active.

No significant variation in microhardness values is observed in the specimens with different α' content. As reported in MARENGO and ALVAREZ [10], there is no evidence of a trend relating microhardness and the extent of the reversion transformation in AISI 316, as opposite to the observations in AISI 304 [2]. As compared with AISI 304, AISI 316 is more stable and hence less DIM is formed by cold work, as shown in column 5 of Table 1. Consequently its hardness is lower than that of 304 and is homogeneous and practically constant in all specimens after the reversion HTs. Perhaps the HTs were not long enough to generate recrystallization or more significant changes in microstructure and mechanical properties of the material.

5. CONCLUSIONS

With the magnetic saturation measurements a new correlation curve for %α' and the feritscope readings (%δ) was obtained, which is also valid for readings higher than 50% and for the assessment of martensite content in steels with a composition (Fe, Cr and Ni) similar to those studied here.

The %α' and permeability curves show that the reversion is active between 400 and 800°C. The permeability value, as an effective parameter from an EC test, is also representative of the amount of magnetic phase. Complete reversion of martensite was not achieved with the 1-hour annealings. There is always some remnant α' which might require longer times to complete the transformation. This might indicate that a diffusion mechanism might be active. Complementary studies should be undertaken in order to understand the decrease in conductivity in the specimens heat treated at higher temperatures.

Metalography of specimens HT up to 700°C are in good agreement with the literature: an α' lath martensite type structure, even for the reverted austenite (γ'). Above 700°C, this type of structure is partially replaced by a finer one, possibly having fewer defects. Further studies are necessary to confirm this hypothesis.

6. ACKNOWLEDGMENTS

7. BIBLIOGRAPHY

[1] DI SCHINO A., KENNY J., "Grain size dependence of the fatigue behaviour of a ultrafine-grained AISI 304 stainless steel", *Materials Letters*, v. 57, pp. 3182–3185, July 2003.

[2] JOHANNSEN D., KYROLAINEN A., FERREIRA P., "Influence of annealing treatment on the formation of nano/submicron grain size AISI 301 austenitic stainless steels", *Metallurgical and Materials Transactions A*, v. 37A, n. 8, pp. 856–890, August 2006.

[3] HEDSTRÖM P., *Deformation and Martensitic Phase Transformation in Stainless Steels*, Doctoral thesis, Division of Engineering Materials Department of Applied Physics and Mechanical Engineering, Luleå University of Technology, Sweden, November 2007.

[4] KNUTSSON A., HEDSTRÖM P., ODÉN M., "Reverse martensitic transformation and resulting microstructure in a cold rolled metastable austenitic stainless steel", Steel *research Int.* v. 79, n. 6, p. 433–439, June 2008.

[5] OLSON G., COHEN M., "A mechanism for the strain-induced nucleation of martensitic transformations", *Journal of the Less-Common Metals*, v. 28, pp. 107–118, 1972.

[6] KESSLER H., PITSCH W.,"On the nature of the martensite to austenite reverse transformation", *Acta Metallurgica*, v. 15, pp. 401–405, February 1967.

[7] KRAUSS Jr G., "Fine structure of austenite produced by the reverse martensitic transformation", *Acta Metallurgica*, v. 11, pp. 499–509, June 1963.

[8] MARENGO J., ALVAREZ P., "Cuantificación del porcentaje de martensita alfa formado durante el maquinado de aceros inoxidables austeníticos de la serie 3xx", In: *I Congreso de Ensayos No Destructivos para América Latina y el Caribe*, San Pablo, Brasil, 21-24 September 1986.

[9] VAN DER PAUW, L., "A method of measuring specific resistivity and Hall effect of discs of arbitrary shape", *Philips Research Reports*, v. 13, pp. 1-9, 1958.

[10] FAVA, J., CARABEDO, F., SPINOSA, C., *Determinación de conductividades en aceros AISI 316 por el método de van der Pauw con evaluación de incertezas*, Report: IN-13-E-150-IN/16 IT, Comisión Nacional de Energía Atómica, Argentina, 2016.

[11] COSARINSKY, G., FAVA, J., RUCH, M., *et al*., "Material characterization by electrical conductivity assessment using impedance analysis", *Procedia Materials Science*, v. 9, pp. 156–162, April 2015.

[12] RUCH, M., FAVA, J., SPINOSA ,C., *et al*., "Characterization of cold rolling-induced martensite in austenitic stainless steels", In: *Proceedings of the 19th World Conference on Non-Destructive Testing 2016*, pp. 13-17, Munich, Germany, June 2016.

[13] LOIS A., RUCH M., "Assessment of martensite content in austenitic stainless steel specimens by eddy currents", In: *BINDT Annual Meeting*; Stratford-Upon-Avon, Inglaterra, 11-14 de September 2006.

[14] TALONNEN, J., ASPEGREN, P., HÄNNINEN, H., "Comparison of different methods for measuring strain induced α' martensite content in austenitic steels", *Mat. Sc. & Technol.*, v. 20, pp. 1506-1512, December 2004.

[15] HECKER S., STOUT M., STAUDHAMMER K., *et al*., "Effect of strain state and strain rate on deformation-induced transformation in 304 stainless steel: Part I. Magnetic measurements and mechanical behavior", *Metallurgical Transactions A*, v.13A, pp. 619-626, April 1982.